

THE SURFACE RADIATION BALANCE IN AND AROUND ARIZONA'S METEOR CRATER

Sebastian W. Hoch and C. David Whiteman

University of Utah, Salt Lake City, Utah, USA

E-mail : shoch@met.utah.edu

Abstract: Topographic influences on the surface radiation balance were studied during the October 2006 Meteor Crater Experiment (METCRAX 2006).

Keywords: Meteor Crater, Arizona, METCRAX 2006, radiation balance, energy balance, net radiation, sidewalls

1. INTRODUCTION

A recent meteorological experiment called METCRAX 2006 (Whiteman et al. 2007, this volume) was conducted in October 2006. This experiment collected extensive radiation data in a unique, idealized topographic basin formed by the impact of a meteorite 50,000 years ago on the Colorado Plateau, 40 km east of Flagstaff, Arizona. The radiation balance is the most important component of the surface energy balance and is the key determinant of the lower boundary condition for all processes that lead to a redistribution of energy within the atmospheric boundary layer. The effects of topography on the radiation balance lead to differing microclimates within mountainous terrain. This article summarizes the radiation data collected as part of METCRAX 2006 and summarizes some of the initial findings.

2. OBSERVATION SITES AND INSTRUMENTATION

Detailed observations of the shortwave and longwave components of the surface radiation budget were made at eight different sites during METCRAX 2006. The geographic locations of the sites are shown in Fig. 1 and listed in Tab. 1. Four of the sites (one on the crater floor, one on the crater rim, and two on the plain outside the crater) were located over quasi-horizontal surfaces. The remaining four sites were located on the sloping crater sidewalls, two on the west slope and two on the east slope.

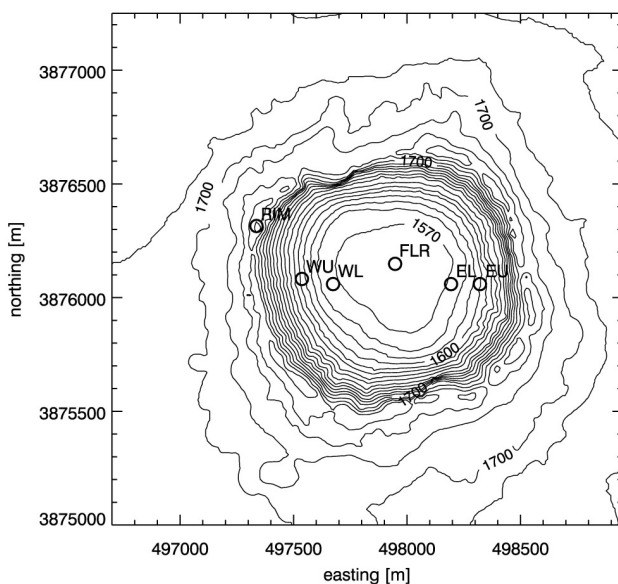


Figure 1: Topographic map showing the radiation sites in the near field of the crater. Two additional sites were located on the Colorado Plateau outside the crater -- the southwest site was 2.5 km SW of the crater center and the ISS site was 5 km NNW of the crater center.

For the six sites in the crater, the four main components of the radiation balance (shortwave incoming, shortwave reflected, longwave incoming and longwave outgoing radiation) were measured individually, parallel to the slope of the underlying terrain, using Eppley PSP or Kipp & Zonen CM21 pyranometers and Eppley PIR or Kipp & Zonen CG4 pyrgeometers. In addition, horizontally oriented REBS Q*7 net radiometers were installed at all sites, with additional slope-parallel Q*7 net radiometers at the sidewall sites. Further, diffuse radiation was measured at the crater rim and floor sites with LiCor pyranometers and shadow-bands. All instrumentation was supplied and installed by the National Center for Atmospheric Research (NCAR). The radiative measurements were made at their Integrated Surface Flux Facilities (ISFF) and Integrated

Sounding System (ISS) sites. Data reported in this paper are 5-min means of data sampled at 5-s intervals. All times are Mountain Standard Time (MST).

Table 1: Radiation measurement site characteristics.

Site Name	Site ID	Longitude (°E)	Latitude (°N)	Altitude (m MSL)	Azimuth (° true)	Slope angle (°)
Crater rim	RIM	-111.0292	35.0295	1744	-	-
Crater floor	FLR	-111.0225	35.0280	1563	-	-
West Upper	WU	-111.0270	35.0274	1609	88	22
West Lower	WL	-111.0255	35.0272	1572	70	4
East Upper	EU	-111.0184	35.0272	1600	264	24
East Lower	EL	-111.0198	35.0272	1572	266	7
Southwest	SW	-111.0388	35.0103	1697	-	-
ISS	ISS	-111.0342	35.0722	1670	-	-

3. THE RADIATION BALANCE ON 21 OCTOBER 2006

The clear day of 21 October 2006 is chosen to illustrate the diurnal variation of the radiative fluxes and the influence of topography. Fig. 2 shows the observed radiative fluxes and inferred variables for the rim and floor as well as the sites located on the crater sidewalls. Tab. 2 shows the radiation totals calculated for the 24-h period beginning at midnight, and for the time period between local sunrise and local sunset. Fig. 3 shows the slope azimuth and elevation angles, sky-view factors, local sunrise and sunset times and duration of direct sunlight, as distributed over the crater.

Table 2: Radiation totals (MJ/m²) calculated from 5-min averages for 21 October 2006. Totals are for the 24-h day from midnight to midnight MST and for the time period between local sunrise and local sunset. NR-h is net radiation for a horizontal radiometer, NR-s is for a slope-parallel radiometer, and NR-c is calculated from 4-components.

Site	Time	ETR	SW in	SW out	SW net	LW in	LW out	LW net	NR-c	NR-s	NR-h	N
FLR	0000-2400	24.37	18.01	3.57	14.44	22.64	32.02	-9.38	5.06	6.42	6.42	288
RIM	0000-2400	24.37	18.84	5.19	13.65	21.18	31.70	-10.52	3.13	5.53	5.53	288
WU	0000-2400	23.79	16.13	3.02	13.11	23.20	32.29	-9.09	4.02	4.61	4.28	288
WL	0000-2400	23.66	16.19	3.10	13.09	22.67	32.43	-9.76	3.33	5.77	5.43	288
EU	0000-2400	25.26	18.02	3.76	14.26	22.68	32.81	-10.13	4.13	4.69	5.43	288
EL	0000-2400	24.62	16.92	3.36	13.56	22.10	32.29	-10.19	3.37	4.43	5.06	288
SW	0000-2400	24.37	-	-	-	-	-	-	-	6.29	6.29	288
ISS	0000-2400	24.37	18.04	-	-	22.02	-	-	-	6.53	6.53	288

Site	Time	ETR	SW in	SW out	SW net	LW in	LW out	LW net	NR-c	NR-s	NR-h	N
FLR	0755-1620	22.61	17.74	3.54	14.20	8.08	13.24	-5.16	9.04	9.41	9.41	101
RIM	0640-1740	24.37	18.84	5.19	13.65	9.69	15.52	-5.83	7.82	8.71	8.71	131
WU	0715-1455	21.99	15.76	2.98	12.78	7.50	11.48	-3.98	8.80	8.48	8.63	92
WL	0735-1525	21.11	15.86	3.05	12.81	7.40	12.18	-4.78	8.03	8.96	8.86	94
EU	0905-1655	23.07	17.64	3.70	13.94	7.43	11.95	-4.52	9.42	8.94	8.93	94
EL	0835-1640	22.35	16.62	3.32	13.30	7.41	12.21	-4.80	8.50	8.63	9.15	97
SW	0640-1740	24.37	-	-	-	-	-	-	-	9.87	9.87	132
ISS	0640-1740	24.37	18.04	-	-	10.13	-	-	-	9.99	9.99	132

4. DISCUSSION

The 21 October data can be compared to measurements made previously in Colorado's Brush Creek Valley (Whiteman et al. 1989) and Switzerland's Riviera Valley (Matzinger et al. 2003).

4.1 Extraterrestrial radiation and sunrise and sunset times

On 21 October, astronomical sunrise and sunset were at 0639 and 1738 MST. The lowest solar zenith angle of 45.88 degrees was reached at 1209 MST. Due to shading by the topography, local sunrise and sunset times varied from site to site. Sunrise at the upper east site was delayed until 0908 MST, while sunset occurred as early as 1453 MST at the upper west site. Sunrise and sunset times throughout the crater are shown in Fig. 3. The crater rim site and both sites on the plain outside the crater, Southwest and ISS, were not significantly obstructed by topography.

4.2 Incoming solar radiation

The incoming solar or global radiation is the sum of direct solar and diffuse radiation. On 21 October, diffuse radiation was 6% of the global radiation, with direct radiation making up the remaining 94%. The effect of the different exposures of the sites (i.e., their slope and azimuth angles) can be seen in Fig. 2. While

global radiation was symmetric about solar noon at the crater floor and rim, the maximum global radiation is received prior to solar noon on the west sidewall and after solar noon on the east sidewall.

4.3 Reflected shortwave radiation and albedo

Albedo at the various sites ranged between 0.19 and 0.21, except at the crater rim, where it was 0.28. This higher albedo is caused by exposed rock surfaces and lack of vegetation. This site is directly illuminated all day and is exposed to the strongest winds.

4.4 Longwave fluxes

Incoming longwave radiation on an unobstructed horizontal surface originates as thermal emissions from the atmosphere and clouds. When higher topography surrounds an observation site, radiation emitted from the surrounding slopes increases the receipt of incoming longwave radiation, since the slopes radiate as black bodies and are at a higher temperature than the effective radiating temperature of the sky. Warmer air above a site also increases incoming radiation. During daytime, warmer air and surrounding terrain lead to higher values of incoming longwave radiation at the slope sites, and lowest values at the crater rim.

4.5 Net radiation

Net radiation was calculated as the sum of the four measured shortwave and longwave in- and outgoing components, but was also measured directly with net radiometers. Large differences between the calculated and directly measured net radiation (Fig. 2, Tab. 2) are thought to be caused by measurement errors with the net radiometers, which are known to have different sensitivities to long- and short-wave radiation and thus require different calibration constants between day and night. Net radiation reaches its minimum shortly after sunset, when the radiating temperature differences between the atmosphere and the surface are greatest. The time of maximum net radiation at a level surface is usually shortly before solar noon, as the net longwave loss is larger after noon. At the slope sites, the time of maximum net radiation is shifted analogously to the incoming shortwave radiation, with a maximum before noon on the west and after noon on the east sidewall.

Net radiation over the 24-hour day varied between 3.13 MJ m^{-2} at the rim and 5.06 MJ m^{-2} at the floor. Thus, 40% less net radiative energy was received at the rim than on the crater floor. This is due to the higher albedo at the rim, and the reduced longwave loss at the crater floor.

At the upper sidewall sites the daily net radiation total amounted to about 4.05 MJ m^{-2} , and at the lower sidewall sites to about 3.35 MJ m^{-2} . Thus, the upper sidewall sites received 21% more net radiative energy than the lower sidewall sites. At the upper east sidewall site, the enhancement (relative to the lower east sidewall site) was due to strong solar insolation on the steeply sloping surface in the afternoon. This enhancement occurred despite the slightly shorter sunlight period at the upper site. At the upper west sidewall site the enhancement (relative to the lower west sidewall site) was caused primarily by the receipt of more downward longwave radiation and, secondarily, by a reduction in outgoing longwave radiation.

5. CONCLUSIONS

The distribution of net radiation within the crater topography shows a remarkable variation which will affect other variables in the surface energy balance, such as latent and sensible heat flux. The spatial variation of the radiation balance depends greatly on the exposure of the crater surface, which determines the shortwave part of the balance, and on the obstruction by surrounding topography, which reduces the longwave energy loss.

Acknowledgements: This research was supported by National Science Foundation grant ATM-0444205. SWH was supported by an Individual Support Fellowship from the Swiss National Science Foundation. We thank the Barringer Crater Company (D. Barringer, Pres.) and Meteor Crater Enterprises, Inc. (B. Andes, Pres.) for crater access, and those listed in the acknowledgments section of Whiteman et al.'s (2007, this volume) METCRAX overview paper for their help with the field program. We especially would like to thank the NCAR field personnel who assisted with the radiation data, including T. W. Horst, W. O. J. Brown, G. Maclean, C. Martin, J. Militzer, S. Oncley, and S. Semmer.

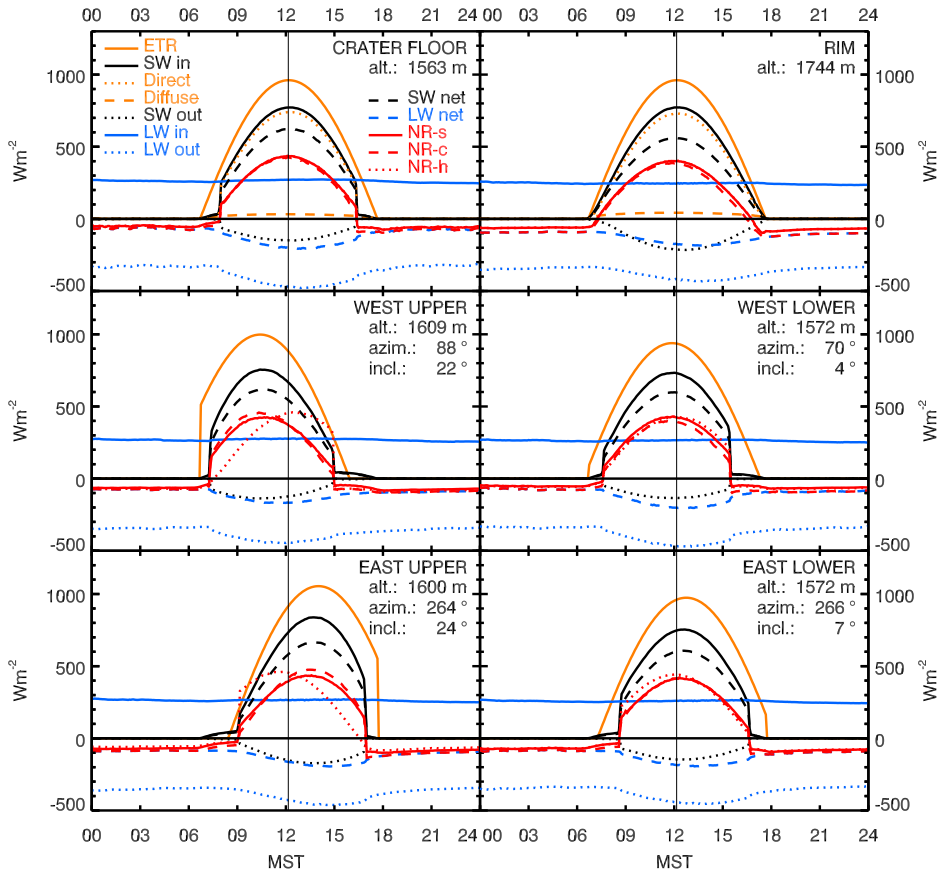


Figure 2: Radiative fluxes observed on 21 October 2006. ETR is extraterrestrial (i.e., theoretical shortwave) radiation, SW is shortwave, LW is longwave. Net all-wave radiation was measured by a slope-parallel net radiometer (NR-s), a horizontal net radiometer (NR-h), or was calculated as the sum of the four individually measured components (Net-c). The thin vertical line denotes solar noon.

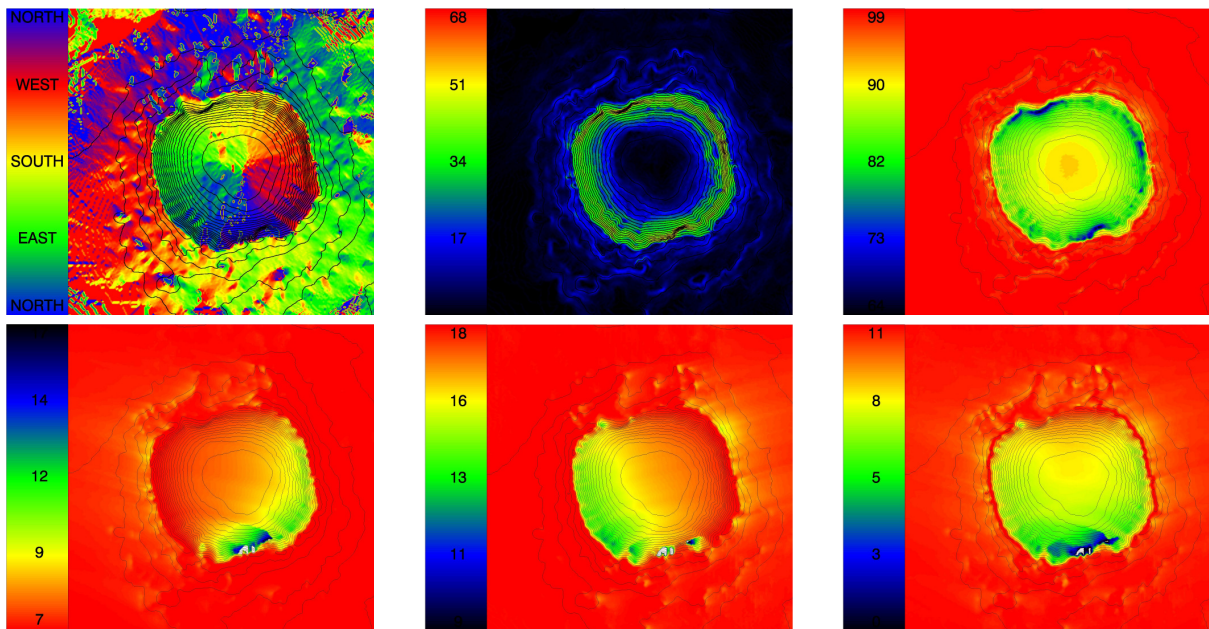


Figure 3: Terrain azimuth (top left), slope inclination angle (top center), sky-view factor (top right), local sunrise time (bottom left), local sunset time (bottom center), and sunshine duration (bottom right) for 21 October 2006.

REFERENCES

- Matzinger, N., M. Andretta, E. Van Gorsel, R. Vogt, A. Ohmura, and M. W. Rotach, 2003: Surface radiation budget in an Alpine Valley. *Quart. J. Roy. Meteor. Soc.*, **129**, 877-895.
- Whiteman, C. D., K. J. Allwine, L. J. Fritschen, M. M. Orgill, and J. R. Simpson, 1989: Deep valley radiation and surface energy budget microclimates. Part I: Radiation. *J. Appl. Meteor.*, **28**, 414-426.